Published in final edited form as:
Brain Res Bull. 2013 February ; 91: 46–51. doi:10.1016/j.brainresbull.2013.01.001.

In vivo SPECT and *ex vivo* autoradiographic brain imaging of the novel selective CB_1 receptor antagonist radioligand [^{125}I]SD7015 in CB_1 knock-out and wildtype mouse

Domokos Máthé[a,b], **Ildikó Horváth**[a], **Krisztián Szigeti**[a,b], **Sean R. Donohue**[c], **Victor W. Pike**[c], **Zisheng Jia**[d], **Catherine Ledent**[e], **Miklós Palkovits**[f], **Tamás F. Freund**[g], **Christer Halldin**[d], and **Balázs Gulyás**[d,*]

[a]Department of Biophysics and Radiation Biology, Semmelweis University, H-1094 Budapest, Hungary

[b]CROmed Translational Research Centers, H-1047 Budapest, Hungary

[c]Molecular Imaging Branch, National Institute of Mental Health, Bethesda, Maryland 20892-2035, USA

[d]Karolinska Institutet Department of Clinical Neuroscience, Psychiatry Section, S-171 76 Stockholm, Sweden

[e]IRIBHM, Université Libre de Bruxelles, Campus Erasme, B-1070 Brussels, Belgium

[f]Laboratory of Neuromorphology, Department of Anatomy, Semmelweis University, H-1094 Budapest, Hungary

[g]Institute of Experimental Medicine of the Hungarian Academy of Sciences, H-1083 Budapest, Hungary

Abstract

We aimed to evaluate the novel high-affinity and relatively lipophilic CB_1 receptor (CB_1R) antagonist radioligand [^{125}I]SD7015 for SPECT imaging of CB_1Rs *in vivo* using the multiplexed multipinhole dedicated small animal SPECT/CT system, NanoSPECT/CT^{PLUS} (Mediso, Budapest, Hungary), in knock-out CB_1 receptor knock-out (CB_1R-/-) and wildtype mice. In order to exclude possible differences in cerebral blood flow between the two types of animals, HMPAO SPECT scans were performed, whereas in order to confirm the brain uptake differences of the radioligand between knock-out mice and wildtype mice, *in vivo* scans were complemented with *ex vivo* autoradiographic measurements using the brains of the same animals. With SPECT/CT imaging, we measured the brain uptake of radioactivity, using %SUV (% standardised uptake values) in CB_1R-/- mice (n = 3) and C57BL6 wildtype mice (n = 7) under urethane anaesthesia after injecting [^{125}I]SD7015 intravenously or intraperitoneally. The Brookhaven Laboratory mouse MRI atlas was fused to the SPECT/CT images by using a combination of rigid and non-rigid algorithms in the Mediso Fusion™ (Mediso, Budapest, Hungary) and VivoQuant (inviCRO,

*Corresponding author at: Karolinska Institutet, Department of Clinical Neuroscience, Psychiatry Section, S-171 76 Stockholm, Sweden. Tel.: +46 8 51770910; fax:+46 8 51771753. balazs.gulyas@ki.se (B. Gulyás).

Boston, MA, USA) softwares. Phosphor imager plate autoradiography (ARG) was performed on 4 μm-thin cryostat sections of the excised brains. %SUV was 8.6 ± 3.6 (average ± SD) in CB_1R-/- mice and 22.1 ± 12.4 in wildtype mice between 2 and 4 h after injection ($p < 0.05$). ARG of identically taken sections from wildtype mouse brain showed moderate radioactivity uptake when compared with the *in vivo* images, with a clear difference between grey matter and white matter, whereas ARG in CB_1R(-/-) mice showed practically no radioactivity uptake. [^{125}I]SD7015 enters the mouse brain in sufficient amount to enable SPECT imaging. Brain radioactivity distribution largely coincides with that of the known CB_1R expression pattern in rodent brain. We conclude that [^{125}I]SD7015 should be a useful SPECT radioligand for studying brain CB_1R in mouse and rat disease models.

Keywords

Endocannabinoid CB_1 receptor (CB_1R); Single photon emission computed tomography (SPECT); Molecular imaging biomarker; [^{125}I]SD7015; Knock-out CB_1R-/- mouse; Multiplexed multipinhole dedicated small animal SPECT/CT system

1. Introduction

The endocannabinoid (EC) system is a widely distributed neuromodulatory system in the brain. The system regulates the functioning of many other neurotransmitter systems, including acetylcholine, dopamine, serotonin, adrenergic, opiate, glutamatergic and GABAergic systems (Freund et al., 2003; Köfalvi et al., 2005; Lambert and Fowler, 2005). The EC system plays a key role in neuronal development (Berghuis et al., 2007; Harkany et al., 2007, 2008; Mulder et al., 2011). One of the main tasks of the central EC system is to mediate the retrograde synaptic communication mainly through type 1 cannabinoid receptors (CB_1R) (Wilson and Nicoll, 2002; Hashimotodani et al., 2007). These receptors show abundant presynaptic expression in the adult mammalian brain (Glass et al., 1997) even though they are also present on the dendrites and soma of neurons but at a lower density than their presynaptic counterparts. They are coupled to Gi/o proteins and, under specific conditions also to Gs proteins (Glass and Felder, 1997). By coupling to Gi/o proteins, CB_1Rs regulate the activity of many plasma membrane proteins and signal transduction pathways, including ion channels, enzymes producing cyclic nucleotide second messengers, and various kinases. In addition CB_1Rs activate G protein-independent pathways (Cannich et al., 2004; Micale et al., 2007; Eljaschewitsch et al., 2006). Several data point to a potent anti-inflammatory and neuroprotective effect of synthetic cannabinoids (Porter and Felder, 2001).

CB_1Rs are relatively abundant in the brain with highest densities in the globus pallidus, lateral caudate putamen, substantia nigra, and cerebellum. Markedly high binding capacities exist in limbic areas (hippocampus, amygdala, cingulate cortex) and the cerebral cortex, especially frontal cortical areas (Glass et al., 1997; Herkenham et al., 1991a,b; Mailleux and Vanderhaeghen, 1992; Westlake et al., 1994; Svízenská et al., 2008). This wide distribution supports the hypothesis that CB_1Rs are implicated in the physiological control of brain mechanisms and functions like learning, memory, cognition, pain perception, appetite, mood, endocrine regulation and motor activity (Breivogel et al., 1999).

Dysfunction of the cannabinoid system has been implicated in many neurological diseases. One of the most widely investigated role of CB_1Rs is nowadays its role in the development of epilepsy. An increasing body of evidence suggests that developmentally increased levels of hippocampal CB_1Rs appear to correlate with epileptogenic activities and epileptogenic developmental pathology (Monory et al., 2006; Ludányi et al., 2008; Magloczky et al., 2010; Zurolo et al., 2010; Karlócai et al., 2011). Several data suggest an important function of ECs to guard against chronic neurodegenerative disorders such as Huntington's disease, Alzheimer's disease and Parkinson's disease (Mulder et al., 2011; Glass et al., 1997; Glass and Felder, 1997; Glass et al., 2000; Di Marzo et al., 2000; Silverdale et al., 2001; Mechoulam et al., 2002; Brotchie, 2003).

In order to investigate alterations in CB_1R density during ageing in various physiological challenge conditions or CNS diseases with *in vivo* or *ex vivo* imaging techniques, high-affinity selective radioligands with good blood–brain–barrier penetration are required. Regarding CB1R imaging with PET there are already a number of available radioligands: [^{11}C]OMAR (Herance et al., 2011; Gao et al., 2012), [^{11}C]CB-119 (Hamill et al., 2009), [^{18}F]MK-9470 (Burns et al., 2007; Casteels et al., 2010a, 2012) as well as [^{11}C]PipISB and [^{18}F]PipISB (Finnema et al., 2009). Regarding SPECT radioligands for CB1Rs, until recently the available battery has been rather limited (Gatley et al., 1998; Lan et al., 1999; Berding et al., 2004; Lindsey et al., 2005). The novel selective high-affinity (K_I = 3.4 nM) and relatively lipophilic (*c*Log*D* = 4.14) CB_1 receptor (CB_1R) antagonist radioligand [^{125}I]SD7015 ([^{125}I]1-(2-iodophenyl)-4-cyano-5-(4-methoxyphenyl)-*N*-(piperidin-1-yl)-1*H*-pyrazole-3-carboxylate), developed recently by some of the present authors (Donohue et al., 2009), appeared to show favourable features in *post mortem* autoradiographic studies in the human brain (Farkas et al., 2012a,b). In order to evaluate this radioligand's *in vivo* imaging capacity, we set out to test it in a small animal mouse model of the intact and impaired central endocannabinoid system, using a cutting-edge small animal SPECT/CT imaging platform.

2. Methods

2.1. Radioligand, radiopharmaceutical kits and chemicals

The detailed synthesis of ([^{125}I]1-(2-iodophenyl)-4-cyano-5-(4-methoxyphenyl)-*N*-(piperidin-1-yl)-1*H*-pyrazole-3 - carboxylate), alias [^{125}I]SD7015, was described in our former publication (Donohue et al., 2009). The specific radioactivity of the ligand was 80.5 GBq/μmol. Tris–HCl, bovine serum albumin (BSA), pargyline hydrochloride (selective MAO-B inhibitor), GBX Developer and Fixer Twin Pack were all purchased from Sigma–Aldrich (Budapest, Hungary). All other chemicals were obtained from commercial sources and were of analytical grade wherever possible.

^{99m}Tc-pertechnetate solution was eluted from a Sorin Drygen technetium generator (Institute of Isotopes Ltd., Budapest, Hungary). Hexamethylpropyleneamine Oxime (HMPAO) for labelling was used in the form of a commercially available radiopharmaceutical kit (Brain-SPECT®, Medi-Radiopharma Ltd., Budapest, Hungary). The kit was reconstituted according to the manufacturer's specifications, with ~2.6 GBq

of ^{99m}Tc-pertechnetate radioactivity in 2.5 mL of physiological saline for each imaging session.

2.2. Animals

CD-1 strain CB_1R knock-out (-/-) mice (CB_1R-/-; *n* = 3) (Ledent et al., 1999) were obtained from the breeding facility of the Institute of Experimental Medicine of the Hungarian Academy of Sciences. Wildtype animals (C57BL6 mice, *n* = 7) were obtained from the Institute of Physiology and Experimental Medicine of Semmelweis University. Mice were kept at the animal housing facility of Semmelweis University's Nanotechnology and *In Vivo* Imaging Centre (NIVIC) under 12/12 L/D light conditions with food and water available *ad libitum*. Animals of the same age (4 months) weighing between 24 and 45 grams were used throughout the studies (mean CB_1R-/-) weight: 40.3 ± 4.5 g, mean C57BL6 weight: 30.2 ± 4.4 g). For imaging, animals were inserted with a 30 G intravenous catheter in their tail vein for providing a continuous intravenous physiological saline infusion (1 mL/animal) during the 120-min-long imaging sessions to prevent dehydration due to the high alcohol content (at least 33% m/v) of the [^{125}I]SD7015 injectate. Throughout the experiments, urethane anaesthesia was used with 10% m/v urethane solution injected i.p. in a dose of 600 mg/kg bodyweight. The experiments were performed in compliance with the relevant EU, Hungarian and university regulations (86/609/EEC/2; Hungarian Act of Animal Care & Experimentation [1998,XXVIII, Section 243/1998]), and permission was provided by the relevant local institutional animal ethics committee.

2.3. In vivo SPECT/CT imaging

Simultaneous dual-isotope SPECT/CT imaging was performed in a dedicated, multiplexed multi-pinhole small animal SPECT/CT imaging system, NanoSPECT/CT^{PLUS} (Mediso, Budapest, Hungary). Iodine-125 and technetium-99m were detected simultaneously with SPECT in three animals (1 wildtype and 2 CB_1R-/-). The detection energy window for^{125}I was set at 25 keV with a 10% difference, while ^{99m}Tc was detected at 140 keV ± 10%. The CT projections were recorded at 55 kV and 170 μA of tube voltage and current, respectively, in the cone-beam CT subsystem of the instrument, with an isotropic voxel size set at 72 μm.

In 8 animals, [^{125}I]SD7015 was administered intravenously (6 wildtypes, 2 CB_1R-/-), whereas in one wildtype and one CB_1R-/-animal the radioligand was administered intraperitoneally. The injected radioactivity dose was 2.3 ± 1.3 MBq in the wildtype mouse and 0.9 ± 0.1 MBq in CB_1R-/- mice (average ± SD), whereas the injected mass was below 20 ng. The imaging session started 120 min after radioligand administration and the data acquisition time was 120 min to allow for adequate signal-to-noise ratio collection in the ^{125}I the imaging channel as the injected iodine radioactivity and brain uptake were low. A total of at least one million counts for the ^{125}I channel were collected in each SPECT session. In the same time in one wildtype mouse 81.0 MBq, in two knock-out mice 78.9 MBq and 41.8 MBq, respectively, ^{99m}Tc-HMPAO solution was administered intravenously 30 min before the start of the imaging session.

2.4. Image analysis

SPECT images were reconstructed from the projection data using the NanoSPECT's HiSpect™ dedicated multiplexing multipinhole reconstruction algorithm (SciVis Ltd, Germany). CT volumes were reconstructed on-the-fly during acquisition of projections, with a Mediso proprietary real-time filtered backprojection algorithm using a Hanning filter with a cut-off at 50%. After reconstructions, the Magnetic Resonance Microimaging Neurological Atlas, developed at the National High-Field Magnetic Resonance Laboratory at the University of Florida (Ma et al., 2005, 2008) was fused to the SPECT/CT images by using a combination of rigid and non-rigid algorithms in the Mediso Fusion™ (Mediso, Hungary) software. Images were further analysed using the Mediso Fusion™ post-processing software. Thus, SPECT/CT/MRI atlas trimodality images were created and used for orientation and regional radioactivity distribution analysis *in vivo*. InVivoScope™ Vivo-Quant software (inviCRO, Boston, MA, USA) was used to determine radioactivity values in Volumes-of-Interest (VOIs). The outcome measure was %SUV (% standardised uptake value):

$$\%SUV = \frac{The\ radioactivity\ in\ the\ target\ organ\ (Bq/\mathrm{g})}{Total\ injected\ radioactivity\ (Bq)\ /body\ weight\ (\mathrm{g})} \times 100$$

For the statistical analysis of the resulting outcome measures (%SUV), due to the small samples sizes, two approaches were used parallel (Wilcoxon–Mann–Whitney rank test, Welch Two Sample *t*-test), whereas the small samples normality values was checked with the Shapiro–Wilk normality test.

2.5. Post mortem autoradiography

The animals were euthanised after the scans and the brains were harvested. Phosphor imager plate autoradiography (ARG) was performed on 4 μm-thin cryostat sections of the excised brains stored on dry ice. A GE Typhoon 9400 (General Electric, USA) imager was used with the sections incubated overnight on the plates, 21 days after imaging.

3. Results

3.1. Cerebral blood flow imaging with HMPAO SPECT

Qualitative analysis of HMPAO SPECT measurements of cerebral blood flow in two CB_1R-/- mice and one wildtype mouse demonstrated no difference between animals, as displayed in characteristic SPECT images (Fig. 1). The quantitative global brain uptake of the radiotracer, measured in %SUV, was 7.2 in the wildtype animal and 4.7 and 8.0 in the CB_1R-/- animals, respectively.

3.2. SPECT imaging with [^{125}I]SD7015

Brain %SUVs between 120 min and 240 min after radioligand administration were 22.1 ± 12.4 (average ± SD) in wildtype mice (n = 7) and 8.6 ± 3.6 in CB_1R-/- mice (n = 3), the difference being significant (Wilcoxon–Mann–Whitney rank test: W = 19, p-value = 0.03333; Welch Two Sample t-test: t = 2.7446, df = 7.176, p-value = 0.02804) (Fig. 2).

Regarding the regional uptake values of the radioligand, the differences between wildtype mice and CB_1R-/- mice proved to be significant in the hippocampus (Wilcoxon–Mann–Whitney rank test: $W = 0$, p-value = 0.01667; Welch Two Sample t-test: $t = 3.4096$, df = 7.045, p-value = 0.01118), but not in other brain structures, despite the fact that, as shown in the images, high uptake of radioactivity was visible in prefrontal, hippocampal and cerebellar areas of the wildtype mouse, whereas in the brain of the knock-out mouse brain, apart from image noise, only the venous sinuses contained appreciable radioactivity.

3.3. Autoradiography with [^{125}I]SD7015

The higher radioactivity uptake regions in the SPECT images of the brains of the wildtype mice occur in CB_1R-rich areas, including the prefrontal cortex, hippocampus and cerebellum. *In vivo* ARG of corresponding sections from wildtype mice displayed moderate radioactivity uptake with a pattern showing higher uptake in grey matter structures and lower uptake in white matter structures, whereas ARG in CB_1R-/-mice showed practically no radioactive uptake in either the *in vivo* SPECT or the *in vivo* ARG image (data not shown).

4. Discussion

CB_1Rs are among the most highly expressed receptors in the vertebrate brain where they play a crucial role in brain development and differentiation; their dysfunction is suspected in many diseases processes. Useful endocannabinoid radioligands for both *in vivo* and *post mortem* neuroimaging studies have long been lacking. [^{18}F]MK-9470 (Van Laere et al., 2008a,b; Casteels et al., 2010b) and [^{11}C]MePPEP (Terry et al., 2009,2010a,b; Donohue et al., 2008) have only recently become available to researchers as useful radioligands for PET imaging. No appropriate radioligand has been available for SPECT studies until the recent development of [^{125}I]SD7015 by some of the present authors (Donohue et al., 2009).

[^{125}I]SD7015 is a novel high-affinity and relatively lipophilic CB_1R antagonist radioligand. The radioligand has been tested in autoradiographic studies using both normal human brain tissue (Donohue et al., 2009) and brain tissue obtained from either Alzheimer's (Farkas et al., 2012a) or Parkinson's disease patients (Farkas et al., 2012b). In all cases, the radioligand effectively visualised CB_1 receptors in the *post mortem* human brain.

In the present study, we used an established knock-out rodent model for testing the brain disposition of radioligands in normal and CB_1R knock-out mouse brains, examined with a nanoScan SPECT/CT scanner. The brain uptake of radioactivity following radioligand administration was significantly lower (practically, the noise level) in the receptor knock-out mice than in the wildtype mice. *Post mortem* autoradiography measurements, performed on brain slices obtained from the same animals, confirmed the observations from imaging.

Considering the cerebral intravascular volume is 5–8% of the total brain volume in the mouse (Chugh et al., 2009), a %SUV value of 5.8 in the mouse brain would indicate basically the intravascular presence of the injected radioactivity only. The values, found with HMPAO, the golden standard to measure cerebral blood volume in SPECT studies, are very close to this "ideal" value (7.2 in one wildtype animal, 4.7 and 8.0, respectively, in the

two CB_1R-/- animals), indicating that indeed HMPAO is a marker of cerebral blood flow. Similarly, the average %SUV value for [^{125}I]SD7015 in the case of the CB_1R-/- animals was very close to this value (8.6 ± 3.6; n = 3). This indicates that radioactivity from this radioligand remains basically in the cerebral vasculature in the brain of these knock-out animals, does not pass the blood–brain barrier, does not enter the brain parenchyma and does not bind to receptors. On the other hand, the average %SUV for [^{125}I]SD7015 in the brains of the wildtype animals was 22.1 ± 12.4, indicating that some radioactivity from this radioligand passed the blood-brain barrier, entered the brain parenchyma and bound to receptors, since radioactivity could be detected there at over two hours after radioligand administration.

5. Conclusion

The present study demonstrates in a rodent model, using CB_1R expressing normal wildtype mice and CB_1R lacking knockout (CB_1R-/-) mice, that [^{125}I]SD7015, the novel high-affinity CB_1 receptor antagonist radioligand can effectively visualise CB_1R populations in the mouse brain with SPECT. Furthermore, as the CB1 neuromodulator system has a rather ubiquitous distribution in the brain of both mice and rats (Pettit et al., 1998; Tsou et al., 1998; Nguyen et al., 2010) and the homology between the receptor protein in rat and mouse is very high (Chakrabarti et al., 1995), the radioligand may also be used successfully in rat disease models, as well. The present observations pave the way for further tests exploring whether [^{125}I]SD7015 or, eventually, its ^{123}I-labelled version, might be used for visualising CB_1Rs in the primate brain.

Acknowledgments

The study was performed partly within a collaborative master research agreement between Karolinska Institutet, Mediso Medical Imaging Systems and CROmed Translational. This study was partially supported by the EU FP7 INMIND Project (Imaging of Neuroinflammation in Neurodegenerative Diseases).

References

Berding G, Müller-Vahl K, Schneider U, Gielow P, Fitschen J, Stuhrmann M, Harke H, Buchert R, Donnerstag F, Hofmann M, Knoop BO, Brooks DJ, Emrich HM, Knapp WH. [^{123}I]AM281 single-photon emission computed tomography imaging of central cannabinoid CB1 receptors before and after Delta9-tetrahydrocannabinol therapy and whole-body scanning for assessment of radiation dose in tourette patients. Biological Psychiatry. 2004; 55:904–915. [PubMed: 15110734]

Berghuis P, Rajnicek AM, Morozov YM, Ross RA, Mulder J, Urbán GM, Monory K, Marsicano G, Matteoli M, Canty A, Irving AJ, Katona I, Yanagawa Y, Rakic P, Lutz B, Mackie K, Harkány T. Hardwiring the brain: endocannabinoids shape neuronal connectivity. Science. 2007; 316(5828): 1212–1216. [PubMed: 17525344]

Breivogel CS, Childers SR, Deadwyler SA, Hampson RE, Vogt LJ, Sim-Selley LJ. Chronic D9-tetrahydrocannabinol treatment produces a time-dependent loss of cannabinoid receptors and cannabinoid receptor-activated G proteins in rat brain. Journal of Neurochemistry. 1999; 73:2447–2459. [PubMed: 10582605]

Brotchie JM. CB1 cannabinoid receptor signalling in Parkinson's disease. Current Opinion in Pharmacology. 2003; 3:54–61. [PubMed: 12550742]

Burns HD, Van Laere K, Sanabria-Bohórquez S, Hamill TG, Bormans G, Eng WS, Gibson R, Ryan C, Connolly B, Patel S, Krause S, Vanko A, Van Hecken A, Dupont P, De Lepeleire I, Rothenberg P, Stoch SA, Cote J, Hagmann WK, Jewell JP, Lin LS, Liu P, Goulet MT, Gottesdiener K, Wagner JA, de Hoon J, Mortelmans L, Fong TM, Hargreaves RJ. [^{18}F]MK-9470, a positron emission

tomography (PET) tracer for in vivo human PET brain imaging of the cannabinoid-1 receptor. Proceedings of the National Academy of Sciences of the United States of America. 2007; 104:9800–9805. [PubMed: 17535893]

Cannich A, Wotjak CT, Kamprath K, Hermann H, Lutz B, Marsicano G. CB1 cannabinoid receptors modulate kinase and phosphatase activity during extinction of conditioned fear in mice. Learning and Memory. 2004; 11:625–632. [PubMed: 15466318]

Casteels C, Bormans G, Van Laere K. The effect of anaesthesia on [(18)F]MK-9470 binding to the type 1 cannabinoid receptor in the rat brain. European Journal of Nuclear Medicine and Molecular Imaging. 2010a; 37:1164–1173. [PubMed: 20182714]

Casteels C, Vanbilloen B, Vercammen D, Bosier B, Lambert DM, Bormans G, Van Laere K. Influence of chronic bromocriptine and levodopa administration on cerebral type 1 cannabinoid receptor binding. Synapse. 2010b; 64(8):617–623. [PubMed: 20340169]

Casteels C, Koole M, Celen S, Bormans G, Van Laere K. Preclinical evaluation and quantification of [^{18}F]MK-9470 as a radioligand for PET imaging of the type 1 cannabinoid receptor in rat brain. European Journal of Nuclear Medicine and Molecular Imaging. 2012; 39:1467–1477. [PubMed: 22699528]

Chakrabarti A, Onaivi ES, Chaudhuri G. Cloning and sequencing of a cDNA encoding the mouse brain-type cannabinoid receptor protein. DNA Sequence. 1995; 5:385–388. [PubMed: 8777318]

Chugh BP, Lerch JP, Yu LX, Pienkowski M, Harrison RV, Henkelman RM, Sled JG. Measurement of cerebral blood volume in mouse brain regions using micro-computed tomography. Neuroimage. 2009; 47(4):1312–1318. [PubMed: 19362597]

Di Marzo V, Hill MP, Bisogno T, Crossman AR, Brotchie JM. Enhanced levels of endogenous cannabinoids in the globus pallidus are associated with a reduction in movement in an animal model of Parkinson's disease. FASEB Journal. 2000; 14:1432–1438. [PubMed: 10877836]

Donohue SR, Krushinski J, Pike VW, Chernet E, Phebus L, Chesterfield A, Felder C, Halldin C, Schaus J. Synthesis, ex vivo evaluation and radio-labeling of potent 1,5-diphenyl-pyrrolidin-2-one cannabinoid subtype-1 (CB1) receptor ligands as candidates for in vivo imaging. Journal of Medicinal Chemistry. 2008; 51:5833–5842. [PubMed: 18800770]

Donohue SR, Varnäs K, Jia Z, Gulyás B, Pike VW, Halldin C. Synthesis and in vitro autoradiographic evaluation of a novel high-affinity radioiodinated ligand for imaging brain cannabinoid subtype-1 receptors. Bioorganic and Medicinal Chemistry Letters. 2009; 19(21):6209–6212. [PubMed: 19767206]

Eljaschewitsch E, Witting A, Mawrin C, Lee T, Schmidt PM, Wolf S, Hoertnagl H, Raine CS, Schneider-Stock R, Nitsch R, Ullrich O. The endocannabinoid anandamide protects neurons during CNS inflammation by induction of MKP-1 in microglial cells. Neuron. 2006; 49:67–79. [PubMed: 16387640]

Farkas S, Nagy K, Palkovits M, Kovács GG, Jia Z, Donohue S, Pike V, Halldin C, Máthé D, Harkany T, Gulyás B, Csiba L. [^{125}I]SD-7015 reveals fine modalities of CB_1 cannabinoid receptor density in the prefrontal cortex during progression of Alzheimer's disease. Neurochemistry International. 2012a; 60(3):286–291. [PubMed: 22222721]

Farkas S, Nagy K, Jia Z, Harkany T, Palkovits M, Donohou SR, Pike VW, Halldin C, Máthé D, Csiba L, Gulyás B. The decrease of dopamine D_2/D_3 receptor densities in the putamen and nucleus caudatus goes parallel with maintained levels of CB_1 cannabinoid receptors in Parkinson's disease: a preliminary autoradiographic study with the selective dopamine D_2/D_3 antagonist [^{3}H]raclopride and the novel CB_1 inverse agonist [^{125}I]SD7015. Brain Research Bulletin. 2012b; 87(6):504–510. [PubMed: 22421165]

Finnema SJ, Donohue SR, Zoghbi SS, Brown AK, Gulyás B, Innis RB, Halldin C, Pike VW. Evaluation of [^{11}C]PipISB and [18F]PipISB in monkey as candidate radioligands for imaging brain cannabinoid type-1 receptors in vivo. Synapse. 2009; 63:22–30. [PubMed: 18925657]

Freund TF, Katona I, Piomelli D. Role of endogenous cannabinoids in synaptic signaling. Physiological Reviews. 2003; 83(3):1017–1066. [PubMed: 12843414]

Gao M, Wang M, Zheng QH. A new high-yield synthetic route to PET CB1 radioligands [^{11}C]OMAR and its analogs. Bioorganic and Medicinal Chemistry Letters. 2012; 22:3704–3709. [PubMed: 22542014]

Gatley SJ, Lan R, Volkow ND, Pappas N, King P, Wong CT, Gifford AN, Pyatt B, Dewey SL, Makriyannis A. Imaging the brain marijuana receptor: development of a radioligand that binds to cannabinoid CB1 receptors in vivo. Journal of Neurochemistry. 1998; 70:417–423. [PubMed: 9422389]

Glass M, Felder CC. Concurrent stimulation of cannabinoid CB1 and dopamine D2 receptors augments cAMP accumulation in striatal neurons: evidence for a Gs linkage to the CB1R. Journal of Neuroscience. 1997; 17:5327–5333. [PubMed: 9204917]

Glass M, Dragunow M, Faull RL. Cannabinoid receptors in the human brain: a detailed anatomical and quantitative autoradiographic study in the fetal, neonatal and adult human brain. Neuroscience. 1997; 77(2):299–318. [PubMed: 9472392]

Glass M, Dragunow M, Faull RLM. The pattern of neurodegeneration in Huntington's disease: a comparative study of cannabinoid, dopamine, adenosine and GABA-A receptor alterations in the human basal ganglia in Huntington's disease. Neuroscience. 2000; 97:505–519. [PubMed: 10828533]

Hamill TG, Lin LS, Hagmann W, Liu P, Jewell J, Sanabria S, Eng W, Ryan C, Fong TM, Connolly B, Vanko A, Hargreaves R, Goulet MT, Burns HD. PET imaging studies in rhesus monkey with the cannabinoid-1 (CB1) receptor ligand [^{11}C]CB-119. Molecular Imaging Biology. 2009; 11:246–252. [PubMed: 19130142]

Harkany T, Guzmán M, Galve-Roperh I, Berghuis P, Devi LA, Mackie K. The emerging functions of endocannabinoid signaling during CNS development. Trends in Pharmacological Science. 2007; 28(2):83–92.

Harkany T, Keimpema E, Barabás K, Mulder J. Endocannabinoid functions controlling neuronal specification during brain development. Molecular and Cellular Endocrinology. 2008; 286(1-2 (Suppl. 1)):S84–S90. [PubMed: 18394789]

Hashimotodani Y, Ohno-Shosaku T, Kano M. Endocannabinoids and synaptic function in the CNS. Neuroscientist. 2007; 13(2):127–137. [PubMed: 17404373]

Herance R, Rojas S, Abad S, Jiménez X, Gispert JD, Millán O, Martín-García E, Burokas A, Serra MÀ, Maldonado R, Pareto D. Positron emission tomographic imaging of the cannabinoid type 1 receptor system with [^{11}C]OMAR ([^{11}C]JHU75528): improvements in image quantification using wild-type and knockout mice. Molecular Imaging. 2011; 10:481–487. [PubMed: 22201539]

Herkenham M, Groen BG, Lynn AB, De Costa BR, Richfield EK. Neuronal localization of cannabinoid receptors and second messengers in mutant mouse cerebellum. Brain Research. 1991a; 552:301–310. [PubMed: 1913192]

Herkenham M, Lynn AB, Johnson MR, Melvin LS, De Costa BR, Rice KC. Characterization and localization of cannabinoid receptors in rat brain: a quantitative in vitro autoradiographic study. Journal of Neuroscience. 1991b; 11:563–583. [PubMed: 1992016]

Karlócai MR, Tóth K, Watanabe M, Ledent C, Juhász G, Freund TF, Maglóczky Z. Redistribution of CB1 cannabinoid receptors in the acute and chronic phases of pilocarpine-induced epilepsy. PLoS One. 2011; 6(11):e27196. [PubMed: 22076136]

Köfalvi A, Rodrigues RJ, Ledent C, Mackie K, Vizi ES, Cunha RA, Sperlágh B. Involvement of cannabinoid receptors in the regulation of neuro-transmitter release in the rodent striatum: a combined immunochemical and pharmacological analysis. Journal of Neuroscience. 2005; 25(11): 2874–2884. [PubMed: 15772347]

Lambert DM, Fowler CJ. The endocannabinoid system: drug targets, lead compounds, and potential therapeutic applications. Journal of Medicinal Chemistry. 2005; 48(16):5059–5087. [PubMed: 16078824]

Lan R, Gatley J, Lu Q, Fan P, Fernando SR, Volkow ND, Pertwee R, Makriyannis A. Design and synthesis of the CB1 selective cannabinoid antagonist AM281: a potential human SPECT ligand. AAPS PharmScience. 1999; 1:E4.

Ledent C, Valverde O, Cossu G, Petitet F, Aubert JF, Beslot F, Böhme GA, Imperato A, Pedrazzini T, Roques BP, Vassart G, Fratta W, Parmentier M. Unresponsiveness to cannabinoids and reduced addictive effects of opiates in CB1 receptor knockout mice. Science. 1999; 283:401–404. [PubMed: 9888857]

Lindsey KP, Glaser ST, Gatley SJ. Imaging of the brain cannabinoid system. Handbook of Experimental Pharmacology. 2005; 168:425–443. [PubMed: 16596783]

Ludányi A, Eross L, Czirják S, Vajda J, Halász P, Watanabe M, Palkovits M, Maglóczky Z, Freund TF, Katona I. Downregulation of the CB1 cannabinoid receptor and related molecular elements of the endocannabinoid system in epileptic human hippocampus. Journal of Neuroscience. 2008; 28(12):2976–2990. [PubMed: 18354002]

Ma Y, Hof PR, Grant SC, Blackband SJ, Bennett R, Slatest L, McGuigan MD, Benveniste H. A three-dimensional digital atlas database of the adult C57BL/6J mouse brain by magnetic resonance microscopy. Neuroscience. 2005; 135(4):1203–1215. [PubMed: 16165303]

Ma Y, Smith D, Hof PR, Foerster B, Hamilton S, Blackband SJ, Yu M, Benveniste H. In vivo 3D digital atlas database of the adult C57BL/6J mouse brain by magnetic resonance microscopy. Frontiers in Neuroanatomy. 2008; 2 http://dx.doi.org/10.3389/neuro.05.001.

Maglóczky Z, Tóth K, Karlócai R, Nagy S, Eross L, Czirják S, Vajda J, Rásonyi G, Kelemen A, Juhos V, Halász P, Mackie K, Freund TF. Dynamic changes of CB1-receptor expression in hippocampi of epileptic mice and humans. Epilepsia. 2010; 51(Suppl 3):115–120. [PubMed: 20618415]

Mailleux P, Vanderhaeghen JJ. Distribution of the neuronal cannabinoid receptor in the adult rat brain: a comparative receptor binding radioautography and in situ hybridization histochemistry. Neuroscience. 1992; 48:655–688. [PubMed: 1376455]

Mechoulam R, Spatz M, Shohami E. Endocannabinoids and neuroprotection. Sci STKE. 2002; 129:RE5. [PubMed: 11972360]

Micale V, Mazzola C, Drago F. Endocannabinoids and neurodegenerative diseases. Pharmacological Research. 2007; 56(5):382–392. [PubMed: 17950616]

Monory K, Massa F, Egertová M, Eder M, Blaudzun H, Westenbroek R, Kelsch W, Jacob W, Marsch R, Ekker M, Long J, Rubenstein JL, Goebbels S, Nave KA, During M, Klugmann M, Wölfel B, Dodt HU, Zieglgänsberger W, Wotjak CT, Mackie K, Elphick MR, Marsicano G, Lutz B. The endocannabinoid system controls key epileptogenic circuits in the hippocampus. Neuron. 2006; 51(4):455–466. [PubMed: 16908411]

Mulder J, Zilberter M, Pasquaré SJ, Alpár A, Schulte G, Ferreira SG, Köfalvi A, Martín-Moreno AM, Keimpema E, Tanila H, Watanabe M, Mackie K, Hortobágyi T, de Ceballos ML, Harkany T. Molecular reorganization of endocannabinoid signalling in Alzheimer's disease. Brain. 2011; 134(4):1041–1060. [PubMed: 21459826]

Nguyen PT, Selley DE, Sim-Selley LJ. Statistical parametric mapping reveals ligand and region-specific activation of G-proteins by CB1 receptors and non-CB1 sites in the 3D reconstructed mouse brain. Neuroimage. 2010; 52:1243–1251. [PubMed: 20451624]

Pettit DA, Harrison MP, Olson JM, Spencer RF, Cabral GA. Immunohistochemical localization of the neural cannabinoid receptor in rat brain. Journal of Neuroscience Research. 1998; 51:391–402. [PubMed: 9486774]

Porter AC, Felder CC. The endocannabinoid nervous system: unique opportunities for therapeutic intervention. Pharmacology and Therapeutics. 2001; 90:45–60. [PubMed: 11448725]

Silverdale MA, McGuire S, McInnes A, Crossman AR, Brotchie JM. Striatal cannabinoid CB1R mRNA expression is decreased in the reserpine-treated rat model of Parkinson's disease. Experimental Neurology. 2001; 169:400–406. [PubMed: 11358453]

Svízenská I, Dubový P, Sulcová A. Cannabinoid receptors 1 and 2 (CB1 and CB2), their distribution, ligands and functional involvement in nervous system structures—a short review. Pharmacology, Biochemistry and Behaviour. 2008; 90(4):501–511.

Terry GE, Liow JS, Zoghbi SS, Hirvonen J, Farris AG, Lerner A, Tauscher JT, Schaus JM, Phebus L, Felder CC, Morse CL, Hong JS, Pike VW, Halldin C, Innis RB. Quantitation of cannabinoid CB1 receptors in healthy human brain using positron emission tomography and an inverse agonist radioligand. Neuroimage. 2009; 48(2):362–370. [PubMed: 19573609]

Terry GE, Hirvonen J, Liow JS, Zoghbi SS, Gladding R, Tauscher JT, Schaus JM, Phebus L, Felder CC, Morse CL, Donohue SR, Pike VW, Halldin C, Innis RB. Imaging and quantitation of cannabinoid CB1 receptors in human and monkey brains using (18)F-labeled inverse agonist radioligands. Nuclear Medicine. 2010a; 51(1):112–120.

Terry GE, Hirvonen J, Liow JS, Seneca N, Tauscher JT, Schaus JM, Phebus L, Felder CC, Morse CL, Pike VW, Halldin C, Innis RB. Biodistribution and dosimetry in humans of two inverse agonists to image cannabinoid CB1 receptors using positron emission tomography. European Journal of Nuclear Medicine and Molecular Imaging. 2010b; 37(8):1499–1506. [PubMed: 20333514]

Tsou K, Brown S, Sañudo-Peña MC, Mackie K, Walker JM. Immunohistochemical distribution of cannabinoid CB1 receptors in the rat central nervous system. Neuroscience. 1998; 83:393–411. [PubMed: 9460749]

Van Laere K, Goffin K, Casteels C, Dupont P, Mortelmans L, de Hoon J, Bormans G. Gender-dependent increases with healthy aging of the human cerebral cannabinoid type 1 receptor binding using [(18)F]MK-9470 PET. Neuroimage. 2008a; 39(4):1533–1541. [PubMed: 18077184]

Van Laere K, Koole M, Sanabria Bohorquez SM, Goffin K, Guenther I, Belanger MJ, Cote J, Rothenberg P, De Lepeleire I, Grachev ID, Hargreaves RJ, Bormans G, Burns HD. Whole-body biodistribution and radiation dosimetry of the human cannabinoid type-1 receptor ligand 18F-MK-9470 in healthy subjects. Journal of Nuclear Medicine. 2008b; 49(3):439–445. [PubMed: 18287275]

Westlake TM, Howlett AC, Bonner TI, Matsuda LA, Herkenham M. Cannabinoid receptor binding and messenger RNA expression in human brain: an in vitro receptor autoradiographic and in situ hybridization histochemistry study of normal aged and Alzheimer's brains. Neuroscience. 1994; 63:637–652. [PubMed: 7898667]

Wilson RI, Nicoll RA. Endocannabinoid signaling in the brain. Science. 2002; 296(5568):678–682. [PubMed: 11976437]

Zurolo E, Iyer AM, Spliet WG, Van Rijen PC, Troost D, Goiter JA, Aronica E. CB1 and CB2 cannabinoid receptor expression during development and in epileptogenic developmental pathologies. Neuroscience. 2010; 170(1):28–41. [PubMed: 20621164]

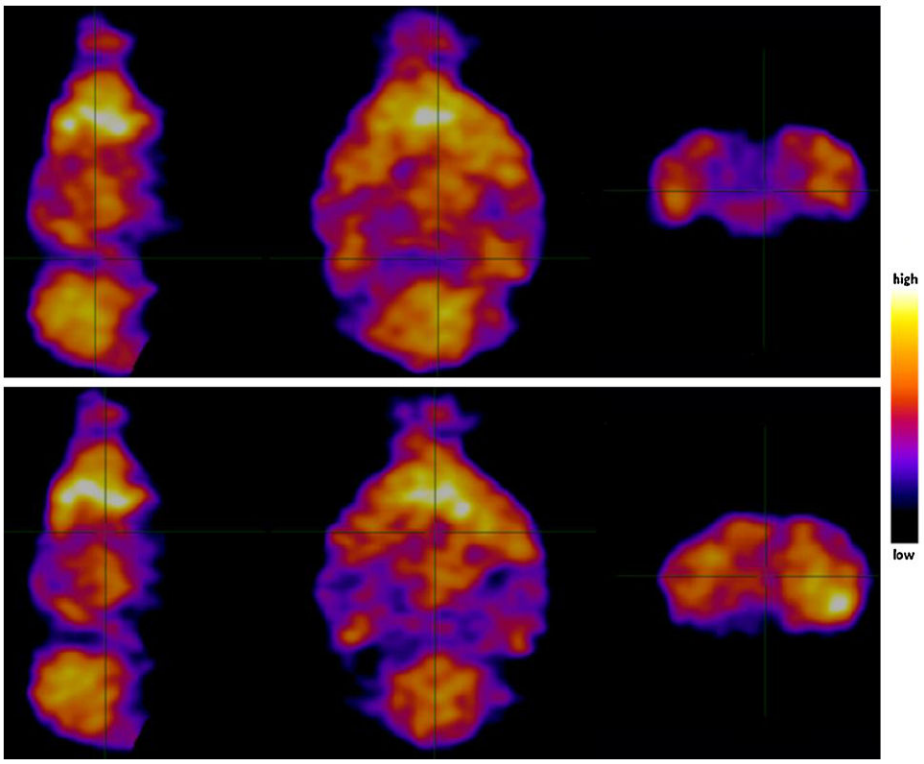

Fig. 1.

Capillary perfusion pattern of the mouse brains imaged with ^{99m}Tc-HMPAO SPECT and CT. One dose of 81.0 MBq of HMPAO radioactivity was injected intravenously into the wildtype mouse (upper row, sagittal, horizontal and coronal slices) and 78.9 MBq into the CB_1R-/- mouse (lower row, sagittal, horizontal and coronal slices). Colour bar (right side) indicate the relative level of cerebral perfusion. The reconstructed SPECT images were co-registered with a high-resolution mouse MRI atlas (MRM NeAT) to allow anatomical identification of radioactivity biodistribution. There is no obvious difference between capillary blood perfusion of CB_1 receptor-expressing and knock-out mouse brains, and thereby a similar input function is assumed.

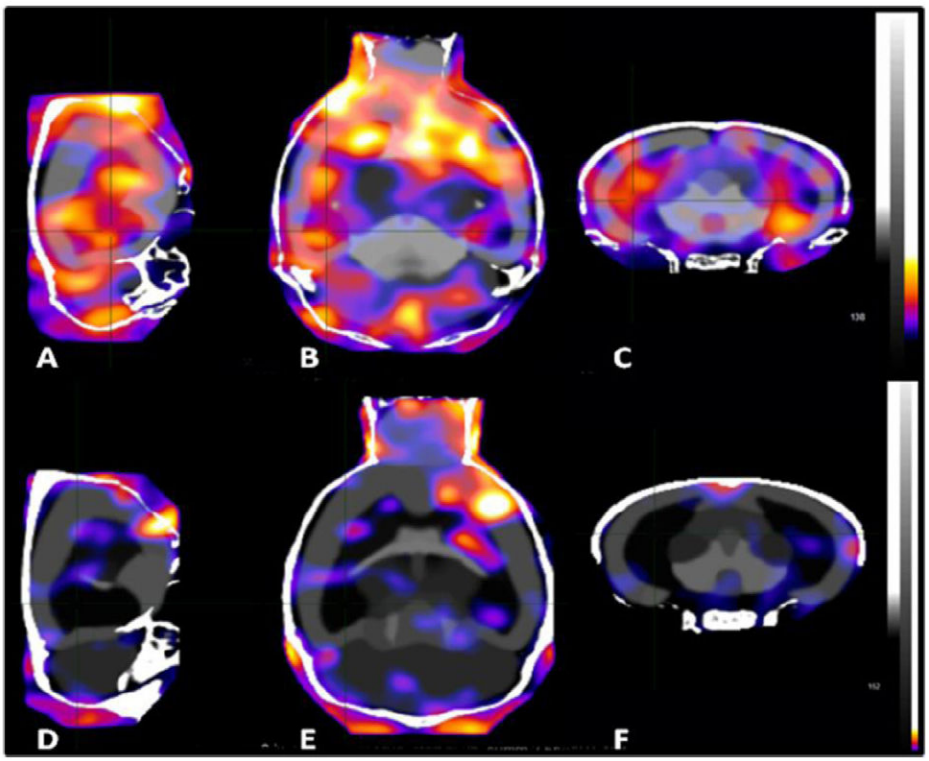

Fig. 2.

A comparison of brain distribution patterns of radioactivity after administrating [^{125}I]SD7015 to wildtype (A–C) and CB_1R-/- mice (D–F). A and D: sagittal images, B and E: horizontal images, C and F: coronal images. Injected radioactivity doses: 0.96 MBq (A–C) and 0.81 MBq (D–F). Average images, data acquisition started 2 h after injection and lasted for 2 h.